Jathushan Kaetheeswaran,
1859 Rosebank Road,
Pickering, Ontario
L1V 1P5
September 14th, 2022

Lisa Aultman-Hall,
Department of Systems Design Engineering

Dear Lisa Aultman-Hall,

I have prepared this report, "Evaluating the effectiveness of artificial intelligence on simulated acoustic angiography data" as my 4A Work Report. This report is the third of three that I must submit as part of my degree requirements. This report was entirely written by me and has not received any previous academic credit at this or any other institution. Prior to this work term, I completed by 3B academic term. The purpose of this report is to examine how artificial intelligence classification algorithms perform binary classification on simulated acoustic angiography data by using accuracy, precision, and sensitivity as performance metrics.

This report topic is an assigned project from the Ultrasound Imaging team at the Sunnybrook research Institute. My supervisor, Dr. Stuart Foster, was responsible for supervising my work term, and is an industry expert that has revolutionized ultrasound technology for healthcare applications. Dr. Foster assigned the project to me due to my extensive experience in software development and my interest in applying this experience towards healthcare research.

I'd like to acknowledge and thank Dr. Foster for supporting me throughout the term and providing bi-weekly feedback for each phase of development during this project. Additionally, I'd like to thank Chris White, Fujifilm VisualSonics' software developer lead, for providing insights into artificial intelligence and how its application can be achieved effectively for our problem space.

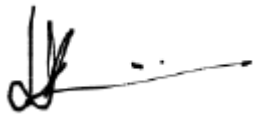

Jathushan Kaetheeswaran,
20768368,
Biomedical Engineering

Evaluating the effectiveness of artificial intelligence on simulated acoustic angiography data

Jathushan Kaetheeswaran
20768368
Biomedical Engineering
Department of Systems Design Engineering, University of Waterloo

This report details the design process for a simulated acoustic angiography generator as well as the engineering analysis of how artificial intelligence classification algorithms perform with binary classification on the simulated data. This project was completed during the Winter and Spring 2022 co-op terms at the Sunnybrook Research Institute. The aim of this project is to provide insights into how machine learning can potentially be incorporated into future ultrasound technology to aid the diagnostic and treatment processes. One of the main undertakings in this project was the modification of existing software, VascuSynth, to generate tumorous vascular networks in an easily reproducible manner such that a large dataset could be generated to train and test a convolutional neural network. This process involved refactoring the existing code repository to prioritize branching that maximized material and power costs, as well as adjusting 3D oxygen demand maps to direct branching towards and away from tumorous regions. The analysis revealed that binary classification of simulated acoustic angiography data can be completed with a high degree of accuracy, sensitivity, and precision. The project was successful in terms of identifying the potential of artificial intelligence algorithms in this field, and future machine learning models can be trained using in-vivo data as well. It is recommended that the tumorous vasculature generator is improved by adding spatial warps to include curvature in the branches, which will improve the realism of the dataset and consequently provide better insights into how the classifications algorithms perform with acoustic angiography data.

Keywords – Acoustic Angiography, Biomedical Simulation, Artificial Intelligence

I. SITUATION OF CONCERN & PROJECT OBJECTIVES

The use of artificial intelligence (AI) for computer-aided diagnoses is an emerging topic in the medical field, as it can significantly improve the efficiency of delivering clinical aid to patients [1]. Emerging machine learning models such as convolutional neural networks (CNNs) have been successful in binary classification with ultrasound scan data, and these same techniques can potentially be applied for classifying acoustic angiography images as well [2].

Acoustic angiography refers to a novel method of ultrasound acquisition involving the injection of microbubbles to act as a contrast agent for dual-frequency transducer imaging [3]. Microbubbles are useful contrast agents in acoustic imaging work because they produce high-frequency responses when excited by low-frequency waves. To capitalize on this, dual-frequency transducers are designed with a low-frequency element that excites the microbubbles, which typically have a resonant frequency below 10 MHz, and a high-frequency element that receives the high-frequency energy returned by the microbubbles. Tracking these microbubbles through post-processing techniques can reveal vascular networks, which are a significant biomarker for cancer research as abnormal structures are often present in malignant tumors and representative of its state.

Incorporating artificial intelligence methods such as CNNs can aid clinical outcomes by providing an automated analysis of these vascular networks in real-time during ultrasound acquisition.

CNNs are deep neural networks that are popular for image classification problems due to the convolutional layers that can extract low-level features initially, such as edges, which are then combined into complex, high-level objects such as bodies [4]. However, CNNs require a large amount of data to train, validate, and test. Acoustic angiography technology is still being developed and improved to acquire high-quality 3D vascular network scans in-vivo, so it is currently not feasible to build a robust CNN with the limited amount of image data available. While the long-term goal is to incorporate machine learning algorithms in the clinical diagnosis process, this project is a proof-of-concept study for evaluating the performance of CNNs using artificial acoustic angiography data. To address this need, this project first details the creation of a pipeline for simulating 3D vascular networks of tumorous and non-tumorous tissue, which is then used to create a robust dataset for validating the use of CNNs in this problem space.

The question for this report is "How do AI classification algorithms perform with binary classification on simulated acoustic angiography data?". The metrics for determining the performance of AI in this problem space are accuracy, precision, and sensitivity which are commonly used performance metrics in machine learning. Success will be determined by these 3-performance metrics, and a high value across all 3 metrics will indicate that AI techniques can be incorporated in clinical use to aid the diagnostic and treatment process.

II. ENGINEERING ANALYSIS

The first goal of this project was to generate realistic 3D vascular trees of both tumorous and non-tumorous trees. Fortunately, existing literature and software provided the means to generate 3D trees of healthy vasculature. The software to simulate this volumetric image data is VascuSynth, published in 2011 by Jassi and Hamarneh from the Medical Image Analysis Lab at Simon Fraser University. VascuSynth was designed with the intention to address the need for vascular tree data to validate segmentation and analysis algorithms [5]. VascuSynth's algorithm follows an iterative growth method where the vascular tree is grown through the connection of existing branches to new terminal nodes [5]. The existing publication and software produced by Jassi and Hamarneh are the basis for the additional work completed in this project - to extend the functionality of VascuSynth to generate tumor vasculature.

VascuSynth generates realistic volumetric image data for healthy vascular trees by following the laws of fluid dynamics such as conservation of flow for bifurcation points, flow, and radii constraints, as well as resistance and pressure changes [5]. Please refer to the original publication for further details on the fluid dynamic equations [5]. However, one of the most valuable features of VascuSynth is that the iterative growth of trees is guided by user-defined oxygen demand maps (ODMs) that can be varied in 3D space. The ODM is a 3D scalar volume that ranges from 0 to 1, representing zero demand and maximum demand respectively. Oxygen demand is important because tumor vasculature is inhomogeneous and chaotic by nature, which causes normal operations such as oxygen supply to be disrupted [6]. Tumors are generally characterized by hypoxia with dense regions of dilated vessels that border areas, towards the center of the tumor, that have low microvasculature density known as necrotic cores [7]. This is the result of the irregular vasculature failing to match the rate at which the tumor cells rapidly proliferate, which

causes cell death and hypoxia [7]. The image from Figure 1, taken from a paper published by researchers at the University of Nice, displays a basic version of this hierarchy [7].

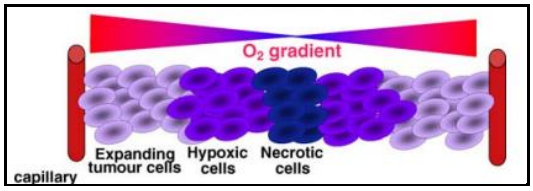

Figure 1. Diagram of how the gradient of oxygen varies throughout a standard tumour mass [*Image Source: MCB, 2007*].

Since hypoxia is a significant biomarker for tumour vasculature, VascuSynth's user defined ODMs provide a unique opportunity to refactor the existing algorithm for healthy vasculature trees and simulate realistic 3D structures of tumour vasculature.

Modifying VascuSynth: Changing the objective function

To build healthy trees using the iterative growth method, VascuSynth's algorithm selects a candidate terminal node from the defined volume, where nodes will be more likely to be selected in regions with higher oxygen demand. This candidate terminal node is then connected to each existing branch in the vascular tree and assigned a fitness value according to the objective function below.

$$Minimize\ [\ \Sigma_{\forall j} L_j^{\mu} r_j^{\lambda}\ ] \qquad (1)$$

The objective function (1) was derived from a 1999 publication from the University of Vienna by Karch et al. and is meant to replicate the geometric and structural optimization that exists in arterial trees to efficiently supply tissues [8]. In this summation, λ and μ are constants that can be changed to create healthy vascular trees with different characteristics, where increasing μ will tend to generate shorter branches while increasing λ will tend to generate branches with small radii [5]. Additionally, L and r represent the length and radius of each of the branches, where j is the index over all existing branches in the tree. The branch that minimizes this function is then permanently connected to the candidate terminal node. This method is suited for geometrical and structural optimization of healthy vascular trees; however, it must be modified to generate tumour vascular trees.

Key characteristics of tumour vasculature must first be identified to design a new objective function. As identified by Rieger et al., tumour vasculature is spatially inhomogeneous with both dense and sparse regions that reflect hypoxic conditions [6]. In addition to the chaotic, tortuous appearance of tumour vasculature, the vessel walls are thin and leaky [6].

The two primary costs to consider for the new function are the material cost and the power cost. Shen et al. detailed the formulas behind these costs in their 2021 publication on the mathematical reconstruction of vascular networks [9]. The material cost is defined by both the materials required for the vessel walls as well as the materials transported through the vessels [9]. The first material cost for endothelial cells can be defined by the surface area of the vessels because these cells line the walls of blood vessels. The second material cost can be defined by the volume of the vessels because it represents the materials in blood such as white and red blood cells, plasma,

etc. Note that both the surface area and volume equations operate under the assumption that vessels are cylindrical. Consequently, Shen et al. define the material cost for a single branch as:

$$MC = 2\pi rl + \pi r^2 l \quad (2)$$

The power cost is defined as the energy that is lost as blood circulates through the vascular network. Shen et al. define the energy loss in a vessel, where μ is the viscosity of blood, as:

$$PC = Q^2 R \quad \text{where } R = \frac{8\mu l}{\Pi r^4} \quad (3)$$

Following the work of Karch et al., these two cost functions will be additive and calculated by indexing over all the existing branches:

$$MC = \sum_{i=0}^{n} (2r_i l_i + r_i^2 l_i) \quad | \quad PC = \sum_{i=0}^{n} (Q^2 \frac{8\mu l}{\Pi r^4}) \quad (4)$$

The relationship between material cost and power cost was examined through experimental trials where it was found that the best qualitative representation of tumor vasculature was generated when the product between these two costs was maximized:

$$Maximize \left[\sum_{i=0}^{n} (2r_i l_i + r_i^2 l_i) * \sum_{i=0}^{n} (Q^2 \frac{8\mu l}{\Pi r^4}) \right] \quad (5)$$

From a physiological perspective, (5) favors trees with the characteristics of tumor vasculature: tortuous, chaotic branching that is inefficient due to leaky vessel walls. Note that the branch which maximizes the material cost (ideally to create tortuous branching), as well as the power cost (to replicate the leaky behavior of vessels), will be chosen to connect to the candidate node. It should be noted that (1) is still used to generate healthy trees as well as healthy sections of tumor networks (such as when a tumor is embedded in a healthy tree).

Hypoxic Region Logic

In addition to changing the objective function, the ODM can be varied to replicate the hypoxic conditions that exist within tumors.

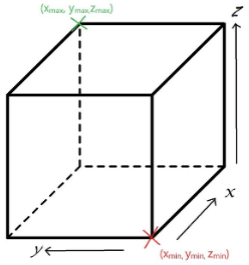

Figure 2. VascuSynth's coordinate system for structuring volumes in 3D space. [*Image Source: JK, 2022*]

VascuSynth accepts ODMs as 3D cubes within the volume with a certain oxygen demand ranging between 0 and 1. To define these 3D cubes, one must define two points:

1. The bottom right corner of the cube
2. The top left corner of the cube

Both these points are defined using X, Y, and Z coordinates. For example, one may define a **100x100x100** volume with constant oxygen demand throughout the entire space:

```
100 100 100
0 0 0 100 100 100
1
```

The snippet above would be used to produce healthy vascular trees because constant oxygen demand throughout the volume produces organized branching. The configuration to include a hypoxic region with a size of **20x20x20** in the center of this volume would be:

```
100 100 100
0 0 0 100 100 100
1
40 40 40 60 60 60
0.5
```

The first 3 digits represent the bottom right corner of the volume, and the last 3 represent the top left corner. The official software guideline for VascuSynth includes further details regarding the configuration files for building vascular trees [5].

Generating Oxygen Demand Maps for Tumor Vasculature

VascuSynth's ability to accept spatially varying ODMs is crucial for generating tumor vasculature embedded within healthy trees. These maps can be manipulated such that the user can freely choose and set where hypoxic and necrotic regions exist within the vascular tree by assigning values to 3D cubes within the main volume as shown in the section prior. The relevance of these values during tree generation is that candidate terminal nodes will be more likely to be chosen in areas with higher oxygen demand (more branching in these areas).

In its current implementation, the modified VascuSynth code generates oxygen demand for tumorous trees using a smooth gradient - the demand decreases by 0.1 from 1 all the way to a region of zero demand (necrotic region). Note that the zero-demand region is necrotic because VascuSynth's logic avoids connecting branches that pass through this region. See the figure below for an example of the random ODMs generated using this method.

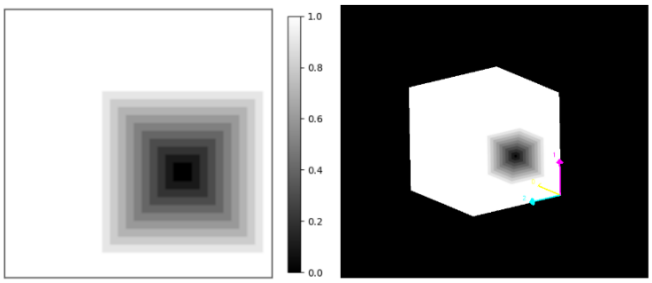

Figure 3. Minimum intensity projection through the z-axis (left), grayscale bar (middle) representing the oxygen demand, and a 3D projection of the total volume's ODM (right). [*Image Source: JK, 2022*]

The result using these modifications is exemplified in the figure below.

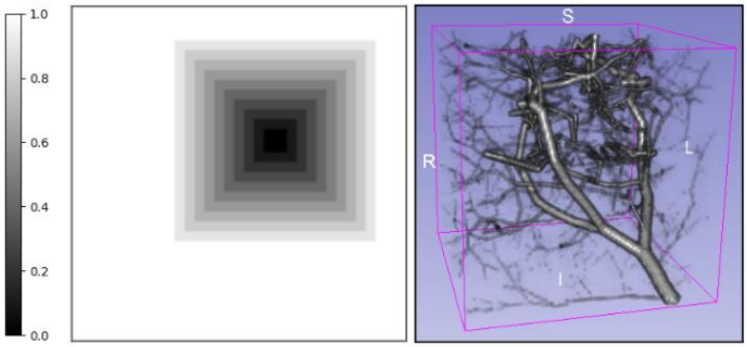

Figure 4. Example of 3D tumor vasculature (right) generated using the modifications from the specified engineering design method. [*Image Source: JK, 2022*]

Generating Maximum Intensity Projections in 360° view

The goal of this project is to evaluate the performance of machine learning models such as CNNs on simulated 3D vasculature, and it is significantly easier for the training, validation, and testing pipeline if the input to the CNN is 2D images. Rather than limit each vascular tree to generating 3 maximum intensity projection images (MIPs) through the X, Y and Z-axis, it would be significantly more efficient to capture images while rotating the vascular tree to obtain more information per tree. This is especially important as the size of the volumes, and consequently, the size of the trees, increases alongside the computational and time costs. To achieve this, a medical image analysis software application called 3D Slicer was used to render the volumes from the 2D slices produced by VascuSynth [10]. Additionally, 3D Slicer supports Jupyter Notebook development, allowing users to code with Python and supporting libraries as well. The Jupyter Notebook file contains logic for uploading the 2D slices from VascuSynth, rendering the 3D vasculature, and displaying the MIP while capturing images. The last step in this methodology is achieved by capturing a single image for every 10° of rotation in the pitch, roll and yaw axis (36 images for 360° of rotation per axis). The image is then degraded with speckle noise to simulate real-world acquisition noise, with a mean of 0 and variance of 0.05. The result of this script is 108 unique MIP images captured for a single vascular tree, which will help to generate large datasets for AI evaluation. See the figure below for an example of several MIP images generated through the pitch axis for a single tumor vasculature volume.

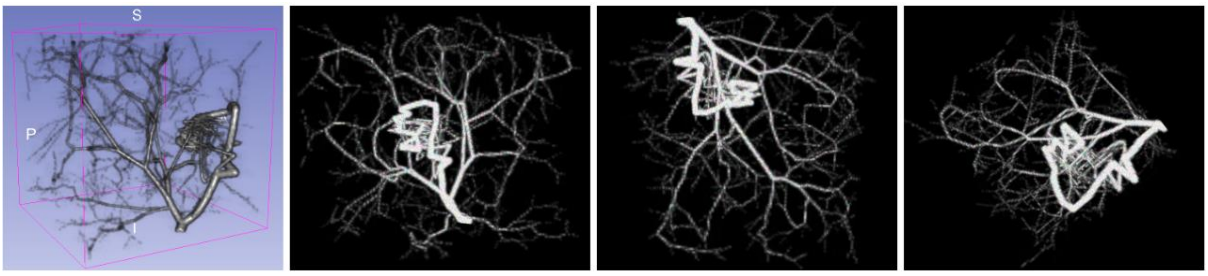

Figure 5. Simulated 3D tumour vasculature in 3D Slicer (left) and MIP images rendered through 3D Slicer and Jupyter Notebook extension (right). [*Image Source: JK, 2022*]

CNN architecture

A simple CNN model was designed to evaluate the performance of machine learning models on the simulated 3D vasculature trees generated previously. This architecture was inspired by the simple CNN model developed by previous work completed by students from the University of Toronto and is comprised of 2 convolutional layers with max-pooling followed by 3 fully connected layers. It should be noted that the original architecture with dropout layers was designed for a dataset containing trees with only 700 nodes. However, after adding more complex trees with 1000 nodes, the dropout layers were no longer necessary. As the dataset grows and incorporates more complex vascular trees, the architecture will likely have to be modified to include more convolutional filters and/or layers for feature extraction. The batch size for this model was 256, the learning rate was 0.0001, and it was trained for 5 epochs.

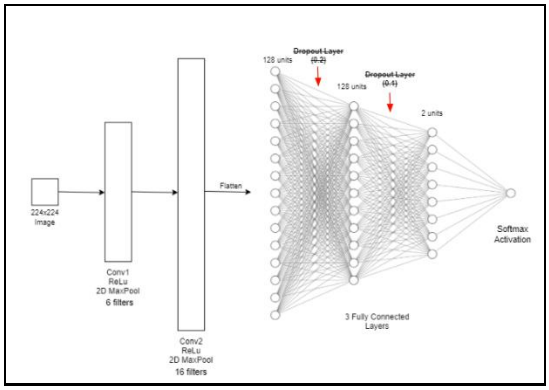

Figure 6. Simple CNN model architecture for binary classification. [*Image Source: JK, 2022*]

III. RESULTS

After applying the logic from the engineering analysis, the pipeline for generating 3D vascular images of non-tumorous and tumorous tissue was complete. A total of 45 trees were generated per class, with 25 of these trees of size 100x100x100 with 700 nodes while the remainder were of size 150x150x150 with 1000 nodes. It should be noted that for future work it would be ideal to generate larger volumes of vascular trees as the number of nodes can also be increased without a large computational cost. Table 1 contains the partition data for the image dataset where the total number of images for each of the training, validation, and test batches were split evenly into 2 classes: tumorous and non-tumorous.

Table 1. Summary of the image dataset and corresponding partitions

	Training	Validation	Test
% of Total Dataset	70	15	15
# of images	6804	1458	1458

The simple CNN model achieved a training accuracy of 95.2% and a validation accuracy of 95.4%. The final training loss was 0.1339 and the final validation loss was 0.1032.

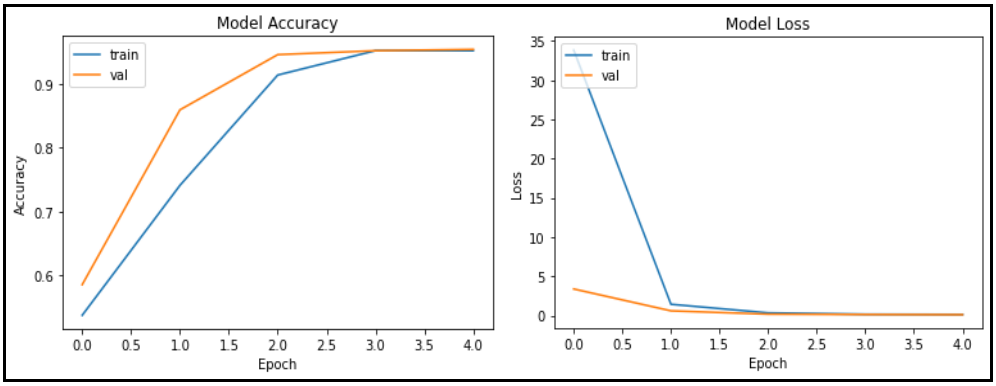

Figure 7. The plot of training and validation accuracy per epoch (left) and plot of training and validation loss per epoch (right). [*Image Source: JK, 2022*]

The CNN was then evaluated using the test set, and the results were plotted to a confusion matrix as shown below. Non-tumorous classifications were considered to be negative, while tumorous classifications were considered to be positive. Consequently, the confusion matrix indicates that the model has a precision of 98.3%, which is the percentage of positive identifications that were correct. The model also has a sensitivity of 94.5%, which is the percentage of true positives that were identified correctly. Finally, the accuracy of the model was 96.4%, which indicates how many samples were correctly classified out of the entire test set.

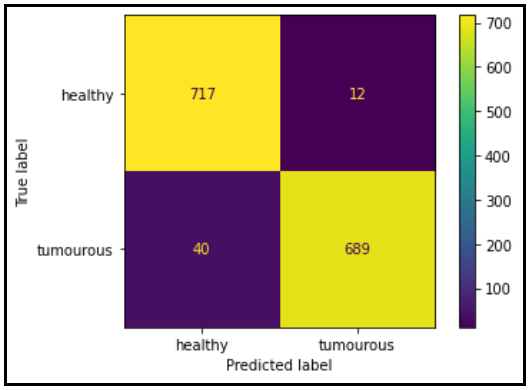

Figure 8. Confusion matrix plot for the performance of the simple CNN on the test set. [*Image Source: JK, 2022*]

IV. DISCUSSION

In the context of clinical diagnosis, it is important to recognize that Type II errors, false negatives, are significantly more detrimental to the health of the patient compared to Type I errors, false positives. This means that the sensitivity rate should be monitored for future development, as this statistic highlights how many tumorous images are being misclassified as non-tumorous by CNN. However, given the simplicity of this model, as well as the small dataset of 9720 total images, the results are promising due to the high precision, sensitivity, and accuracy values. Although the sensitivity rate is slightly lower than precision and accuracy, it is nevertheless above 90% which is a successful percentage in the machine learning community. Therefore, it can be said that AI classification algorithms are able to perform binary classification very well on simulated acoustic angiography data.

V. LIMITATIONS OF DESIGNED SOLUTION

The main limitation of the designed solution is that it relies on existing software that has been published for simulating healthy vascular trees. This software was published in 2011, and as a result, there are limited up-to-date resources for interfacing with the code repository. From my own experience, this resulted in a significant time cost for modifying the existing software to produce realistic vascular trees. Therefore, future work will be impacted by the onboarding process required for new developers to understand the system and modify it for generating tumorous vascular trees. Additionally, relying on existing software can be potentially problematic as certain logic that has been integrated into the system requires a large amount of time and effort to rework, such as the algorithms required for linear branching. If a developer wanted to change this logic to include branches with curvature, this would require them to refactor several complex C++ files that were published by a third-party of researchers. The project was successful despite these limitations because I have a significant amount of experience refactoring existing code repositories, which helped to reduce troubleshooting concerns throughout the development process.

VI. CONCLUSIONS

In summary, this project was a successful proof-of-concept for the use of machine learning algorithms in classifying simulated images of 3D tumorous and non-tumorous vasculature. While the final pipeline will have to include training on real-world ultrasound angiography images, this project highlights the potential to train and develop machine learning models using simulated 3D vasculature images to account for the lack of available datasets in this field. The development of dual-frequency array transducers, microbubble agents, and bubble tracking software is currently progressing, and the point at which this project intersects with real-world acquisitions will provide new insights into the use of AI in ultrasound angiography.

VII. RECOMMENDATIONS

Recommendation

With respect to the generator, one major area of improvement would be to apply a deformable, B-spline spatial warp, as performed by the original VascuSynth authors, to get rid of linear branches with sharp angles that are not realistic [5].

Rationale

The images below highlight how this spatial warp can dramatically improve the realism of the vasculature, and while the original authors did not provide the source code for this operation,

this addition to the existing logic would allow for more rigorous testing of AI models for the purposes of acoustic angiographies.

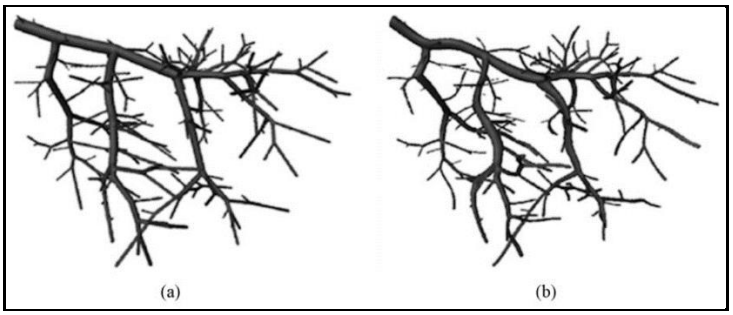

Figure 9. Images provided by Hamarneh and Jassi for non-tumorous vasculature with a) linear branching and b) spatially warped branching. [*Image Source: GH, 2011*]

Costs

Applying a deformable, B-spline spatial warp to the existing VascuSynth code repository is a significant undertaking that will likely take 1-2 months. The major factor is this estimate is how familiar the user is with working with C++ code and how comfortable they are with applying spatial warps to linear branches in 3D space. There are existing publications regarding the application of image warping algorithms for 3D models, and these could be used a starting point for development. The employees who are tasked with this job will have to be financially compensated as well as receive the necessary training to interface efficiently with the available software tools.

Benefits

The benefit of this addition to the existing simulation software is that there is improved realism integrated into the dataset generator. The importance of this is that a more realistic dataset will help to better evaluate how AI algorithms are able to classify complex vascular networks. As this work is one part of a multi-year research project, improving the simulated acoustic angiography data will be valuable to future work regarding the effectiveness of AI in this field.

ACKNOWLEDGMENTS

Many thanks to Dr. Stuart Foster and Dr. Christine Démoré at the Sunnybrook Research Institute for supervising this 8-month project and providing bi-weekly feedback. Many thanks to Chris White and Fujifilm VisualSonics for assisting with the machine learning portions of this project and providing expertise in the ultrasound angiography field.

REFERENCES

[1] A. Singh, S. Sengupta, and V. Lakshminarayanan, "Explainable deep learning models in medical image analysis," Journal of Imaging, vol. 6, no. 6, p. 52, 2020.

[2] M. C. Walker, I. Willner, O. X. Miguel, M. S. Murphy, D. El-Chaâr, F. Moretti, A. L. Dingwall Harvey, R. Rennicks White, K. A. Muldoon, A. M. Carrington, S. Hawken, and R. I. Aviv, "Using deep-learning in fetal ultrasound analysis for diagnosis of cystic hygroma in the first trimester," PLOS ONE, vol. 17, no. 6, 2022.

[3] R. C. Gessner, C. B. Frederick, F. S. Foster, and P. A. Dayton, "Acoustic angiography: A new imaging modality for assessing microvasculature architecture," *International Journal of Biomedical Imaging,* vol. 2013, pp. 1–9, 2013.

[4] S. Albawi, T. A. Mohammed, and S. Al-Zawi, "Understanding of a convolutional neural network," 2017 International Conference on Engineering and Technology (ICET), 2017

[5] G. Hamarneh and P. Jassi, "Vascusynth: Simulating vascular trees for generating volumetric image data with ground-truth segmentation and tree analysis," Computerized Medical Imaging and Graphics, vol. 34, no. 8, pp. 605–616, 2010.

[6] H. Rieger, T. Fredrich, and M. Welter, "Physics of the tumor vasculature: Theory and experiment," The European Physical Journal Plus, vol. 131, no. 2, 2016.

[7] M. C. Brahimi-Horn, J. Chiche, and J. Pouysségur, "Hypoxia and cancer," Journal of Molecular Medicine, vol. 85, no. 12, pp. 1301–1307, 2007.

[8] R. Karch, F. Neumann, M. Neumann, and W. Schreiner, "A three-dimensional model for arterial tree representation, generated by constrained constructive optimization," Computers in Biology and Medicine, vol. 29, no. 1, pp. 19–38, 1999.

[9] J. Shen, A. H. Faruqi, Y. Jiang, and N. Maftoon, "Mathematical reconstruction of patient-specific vascular networks based on clinical images and global optimization," IEEE Access, vol. 9, pp. 20648–20661, 2021.

[10] "About 3D Slicer," 3D Slicer image computing platform. [Online]. Available: https://slicer.readthedocs.io/en/latest/. [Accessed: 18-Aug-2022].

Sources of Images

Images presented in this document created by the authors are indicated by author initials and year of creation.

M. C. Brahimi-Horn, J. Chiche, and J. Pouysségur, "Hypoxia and cancer," Journal of Molecular Medicine, vol. 85, no. 12, pp. 1301–1307, 2007.

G. Hamarneh and P. Jassi, “Vascusynth: Simulating vascular trees for generating volumetric image data with ground-truth segmentation and tree analysis,” Computerized Medical Imaging and Graphics, vol. 34, no. 8, pp. 605–616, 2010.